

# Chemical Solution Deposition of PZT/Oxide Electrode Thin Film Capacitors and Their Micro-patterning by using SAM

Hisao Suzuki<sup>1</sup>

Dept. of Materials Science, Shizuoka University, Hamamatsu, Shizuoka, Japan

## Abstract

*Micro-patterns of  $Pb(Zr_{0.53}Ti_{0.47})O_3$ , PZT, thin films with a MPB composition were deposited on Pt/Ti/SiO<sub>2</sub>/Si substrate from molecular-designed PZT precursor solution by using self-assembled-monolayer(SAM) as a template. This method includes deposition of SAM followed by the optical etching by exposing the SAM to the UV-light, leading to the patterned SAM as a selective deposition template. The pattern of SAM was formed by irradiating UV-light to the SAM on a substrate and/or patterned PZT thin film through a metal mask for the selective deposition of patterned PZT or lanthanum nickel oxide (LNO) precursor films from alkoxide-based precursor solutions. As a result, patterned ferroelectric PZT and PZT/LNO thin film capacitors with good electrical properties in micrometer size could be successfully deposited.*

## 1. Introduction

Lead zirconate titanate(PZT) thin films have been attracting worldwide interests in exploring their potential properties [1-3] or the origins [4-6] of their excellent dielectric, ferroelectric and piezoelectric properties near the morphotropic phase boundary (MPB). PZT thin films are expected to apply to the memory devices, micro electro mechanical systems (MEMS), and display because of their superior ferroelectric, pyroelectric, piezoelectric and electron emission properties. Advancement of the nanotechnologies requires the ultra-fine processing to develop novel devices, and wet etching through the register [7], reactive ion etching [8], sputtering through the mask [9], electron beam lithography [10], laser cutting [11] and others are proposed for ultra-fine processing of PZT thin film capacitors on Si wafers. However, these techniques are relatively complex and, therefore, are expensive as well as the problem for etching rate. Thus, we propose a novel ultra-fine processing for selective deposition of thin films on intended area in micrometer size. This method includes deposition of self-assembled-monolayer (SAM) [12]. SAM is organic molecule

film covering solid surfaces spontaneously with well-ordered and oriented molecules, exposing specific functional groups outside which can modify surface properties. This paper describes the deposition of patterned PZT and PZT/LNO thin film capacitors using SAM molecule with both fluoride chain and thiol group in one molecule for Pt electrode or using SAM molecule with SiCl<sub>3</sub> in the end of molecule, so called, octadecyl-trichloro-silane (OTS) for patterned PZT film.

We also focus the electrical properties of the resultant patterned PZT and PZT/LNO thin film capacitors so as to assess the applicability for devices.

## 2. Experimental Procedure

In this study, SAM molecule, CF<sub>3</sub>(CF<sub>2</sub>)<sub>5</sub>C<sub>13</sub>H<sub>24</sub>O<sub>2</sub>SH, which had fluoride chain and thiol group in one molecule and SAM molecule with SiCl<sub>3</sub> in the end of molecule, so called, octadecyl-trichloro-silane (OTS) were used to control the wettability. The molecule of CF<sub>3</sub>(CF<sub>2</sub>)<sub>5</sub>C<sub>13</sub>H<sub>24</sub>O<sub>2</sub>SH was synthesized by dehydration condensation between 3,3,4,4,5,5,6,6,7,7,8,8,8-tridecafluoro-1-octanol and 11-mercaptoundecanoic acid using N,N-dicyclohexylcarbodiimide as dehydration reagent. On the other hand, commercially available octadecyl-trichloro-silane (OTS) was used for the patterning of LNO upper electrode film to improve the electrical fatigue properties.

Trihydrated lead acetate, titanium iso-propoxide and zirconium n-propoxide were used as starting materials, and absolute ethanol was used as a solvent to prepare the CSD precursor solution. The Zr/Ti ratio was 53/47, and excess Pb (20 mol%) was added to the solution. The nominal composition of the precursor solution was equivalent to that of Pb<sub>1.2</sub>(Zr<sub>0.53</sub>Ti<sub>0.47</sub>)O<sub>3</sub>. Details of the precursor solution preparation are described elsewhere [13]. The concentration of the PZT precursor solution was controlled at 0.5 M.

Patterning of PZT thin films were carried out using SAM molecule and PZT precursor solution. At first, Pt(111)/Ti/SiO<sub>2</sub>/Si substrate was dipped in SAM precursor solution. Next, the SAM template was

created by exposing SAM to ultraviolet ray through the metal mask (SAM patterning process). After SAM patterning process, PZT precursor was dip-coated. A sequence of SAM patterning process, dip coating of PZT precursor film, drying at 115 °C, pyrolysis at 350 °C for 10min and annealing at 550 °C were repeated to increase the film thickness (patterning process). Final annealing was performed at 700 °C for 2h in air.

Crystalline phases in the patterned PZT thin film were identified by X-ray diffraction (XRD). For electrical measurement, Au top electrode was sputtered through the metal mask with 100 $\mu$ m circular holes. Oxide thin film electrode of LNO was also patterned by using OTS SAM as a same manner of PZT film patterning for the patterned PZT thin film. The details of the LNO precursor solution was described elsewhere [14]. Dielectric behavior of the patterned PZT thin film was measured by LCR meter (HP-4284A). P-E hysteresis loops and the fatigue property for the resultant patterned thin film capacitors were measured by RT6000S (Radiant Technology Inc.).

### 3. Results and Discussion

#### 3.1 Deposition of Patterned PZT Film

Figure 1 shows wettability (water affinity) change for Pt(111)/Ti/SiO<sub>2</sub>/Si substrate after dipping into the CF<sub>3</sub>(CF<sub>2</sub>)<sub>5</sub>C<sub>13</sub>H<sub>24</sub>O<sub>2</sub>SH SAM with exposing time to the UV light. This figure demonstrated that the wettability of Pt(111)/Ti/SiO<sub>2</sub>/Si substrate could be effectively controlled by using the originally prepared thiol SAM. Figure 2 shows the optical microscope image of patterned PZT thin films. As shown in Fig. 2, uniform patterned 700 $\times$ 700 $\mu$ m PZT thin films could be deposited on the silicon wafer. The deposited PZT patterns exhibited same shape and size with those of the metal masks used. This result exhibited the high potential of CF<sub>3</sub>(CF<sub>2</sub>)<sub>5</sub>C<sub>13</sub>H<sub>24</sub>O<sub>2</sub>SH as a SAM, and this SAM molecule has the following three excellent features; (1) SH group in a SAM molecule reacts easily with metal to form strong chemical bonding. In case of this study, SAM forms only by dipping the substrate in CF<sub>3</sub>(CF<sub>2</sub>)<sub>5</sub>C<sub>13</sub>H<sub>24</sub>O<sub>2</sub>SH solution because SH group reacts platinum as electrode on the surface of substrate [15]. (2) Although the mechanism of chemical adsorption of the sulfur on the surface of metal is not well understood, it has been proposed that an organic compound adsorbs as metal thiolate(RS<sup>-</sup>M<sup>+</sup>) on metal surface [16, 17]. This chemical bonding can easily decompose by irradiating the ultraviolet ray because

the energy of ultraviolet ray exceeds that of the metal thiolate chemical bonding [18]. Therefore in this study, Pt-S chemical bonding also can be decomposed by ultraviolet ray irradiation, leading to the easy formation of patterned SAM template by ultraviolet ray irradiation through the metal mask. (3) The third feature is the suppression of chemical reaction between PZT precursor solution and Pt electrode due to fluoride chain. The contact angle of the PZT precursor solution on SAM was 112°. On the other hand, the contact angle of the PZT precursor solution on the substrate after ultraviolet ray irradiation was 172°. Because SAM molecule was decomposed after pre-annealing at 350 °C, the same SAM template and same PZT precursor pattern can be easily deposited repeatedly to increase the thickness of the patterned PZT thin film by repeating the patterning process.

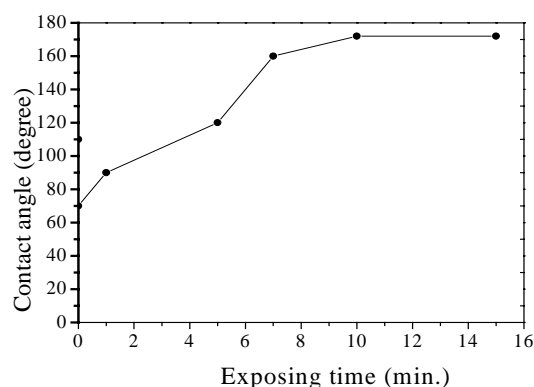


Fig. 1 Wettability change for the thiol SAM modified Pt(111)/Ti/SiO<sub>2</sub>/Si substrate with exposing time to UV light.

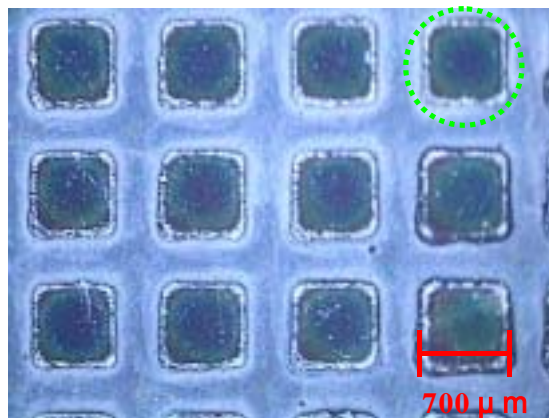


Fig. 2 Optical microscope image of the patterned PZT thin film.

### 3.2 Characterization of Patterned PZT Thin Film

Figure 3 shows XRD pattern for the patterned PZT film. The XRD pattern shows perovskite structure except for the Pt (111) and Pt(200) peaks. This result shows that patterned PZT thin film of a single phase perovskite structure with mainly (111)-orientation was able to be obtained by this patterning process and a SAM template did not affect both on the crystal structure and film orientation, because a SAM molecule decomposed before crystallization of a perovskite PZT.

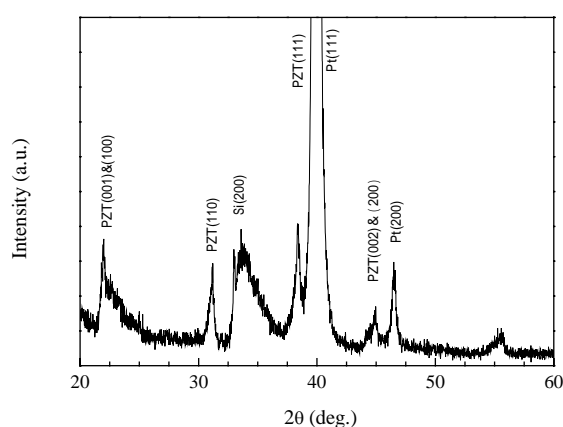


Fig. 3 XRD pattern for the patterned PZT thin film.

Figures 4 and 5 show the dielectric and the ferroelectric properties for the patterned PZT film, together with those for the non-patterned PZT film by comparison. As shown in Fig.3, dielectric behavior of the patterned PZT thin film was almost same as that of the non-patterned PZT thin film except for the relatively large loss at low frequencies. This may be ascribed to the increased grain boundaries. Non-patterned PZT thin film was deposited from same solution and by same annealing process. High potential for a micro-patterning with SAM was confirmed by the P-E hysteresis loops for the patterned and non-patterned PZT films in Fig.4, showing almost same ferroelectric properties. These results demonstrates that micro-patterning of PZT thin films with SAM as a template using  $\text{CF}_3(\text{CF}_2)_5\text{C}_{13}\text{H}_{24}\text{O}_2\text{SH}$  molecule is very useful as a novel and easy fine processing technique for oxide thin films with chemical solution deposition (CSD).

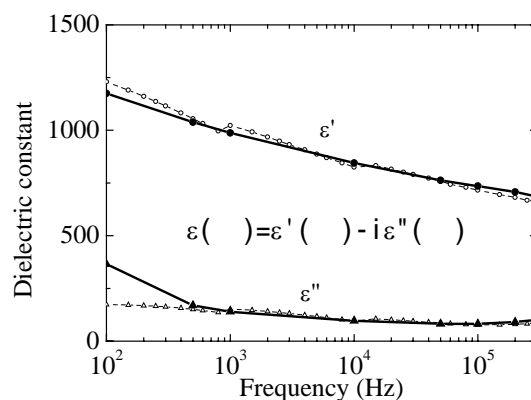


Fig. 4 Dielectric properties for the patterned PZT thin film compared with that for the non-patterned PZT thin film.

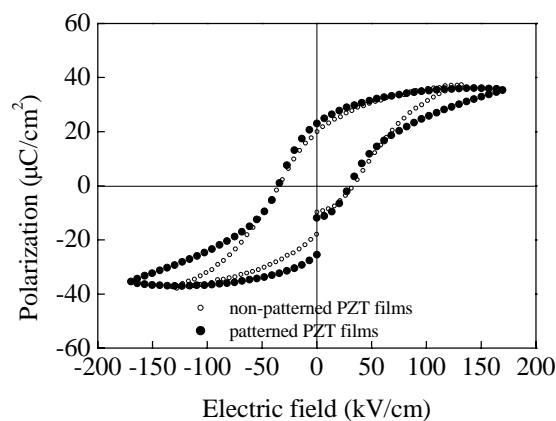


Fig. 5 Ferroelectric properties for the patterned PZT thin film compared with that for the non-patterned PZT thin film.

### 3.3 Orientation Control of Patterned PZT Film by Seeding Layer

For the better electrical properties of the resultant thin film patterns, orientation control of the PZT thin film is essential. Therefore, orientation control of the patterned PZT thin film was tried by inserting the PbO seeding layer (Fig.6). Orientation mechanism was described elsewhere [19]. As a result, highly

(100)&(001)-oriented patterned PZT thin film was successfully deposited. The degree of the orientation was calculated to be about 79 %. Figure 7 shows cross-sectional SEM image for the (100)&(001)-oriented patterned PZT thin film. As can be seen in Fig. 7, the surface of the (100)&(001)-oriented patterned PZT was relatively smooth and the film was consisted of the relatively granular grains, leading to the imperfect orientation..

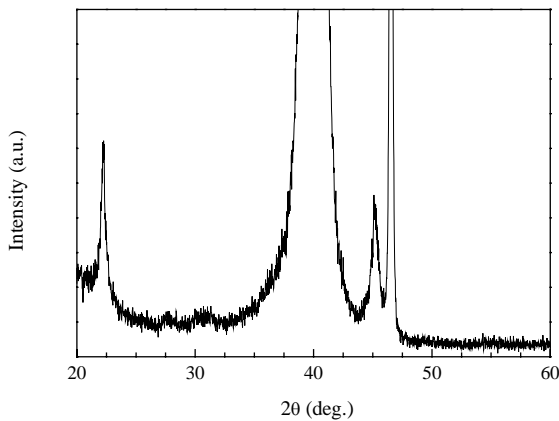


Fig. 6 XRD pattern for the patterned PZT thin film deposited on the patterned PbO seeding layer.

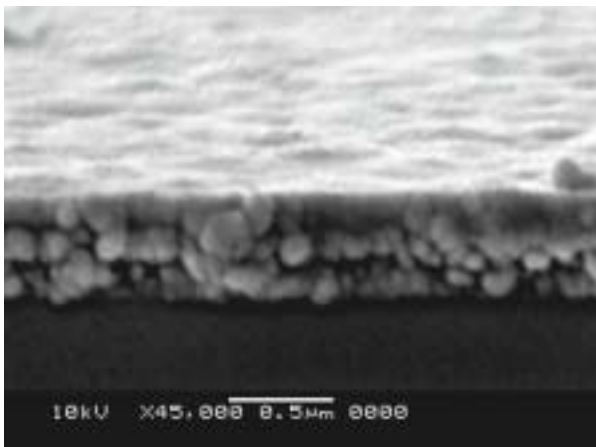


Fig. 7 SEM image for the patterned PZT thin film deposited on the patterned PbO seeding layer.

### 3.4 Deposition of Patterned LNO Film on Patterned PZT Film

To improve the electrical fatigue for the PZT thin film, use of a perovskite-type oxide thin film electrode is very effective. Therefore in this study, lanthanum nickel oxide (LNO) thin film was also patterned by using octadecyl-trichloro-silane (OTS) SAM. OTS SAM is the molecules with  $\text{SiCl}_3$  in the end of molecule and can react with OH group on the substrate surface to form Si-O-Si bonding. Therefore, this SAM can be used on the surface of the oxide thin film with enough OH group such like PZT thin film. However, OTS SAM did not form on the surface of the crystallized PZT thin film because of the lack of enough amount of OH group. Then, we formed OTS SAM on the surface of the pre-annealed patterned PZT thin film according to the following procedure illustrated in Fig.8.

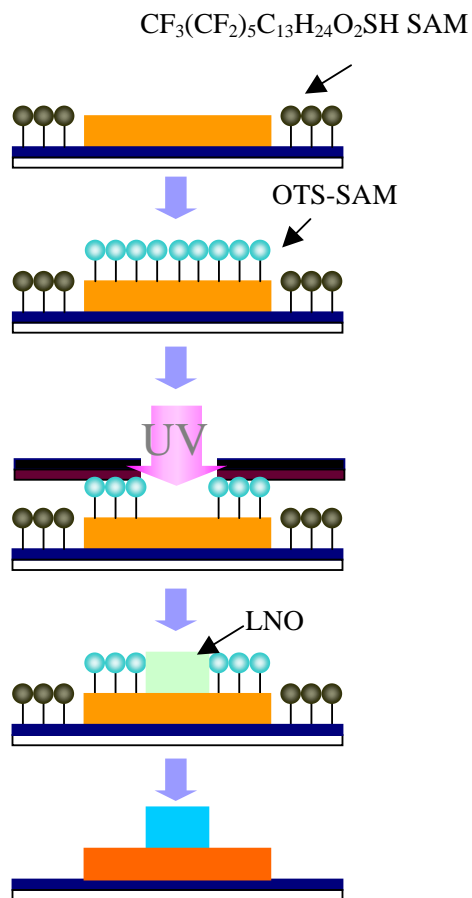


Fig. 8 Deposition process for patterned LNO film.

As a result, we successfully deposited patterned PZT/LNO thin film capacitor as shown in Fig. 9. The size of the LNO thin film pattern could be reduced to about 100 micron. This size will be reduced to about several micron if the very thin metal mask is used as well as the PZT thin film patterns.

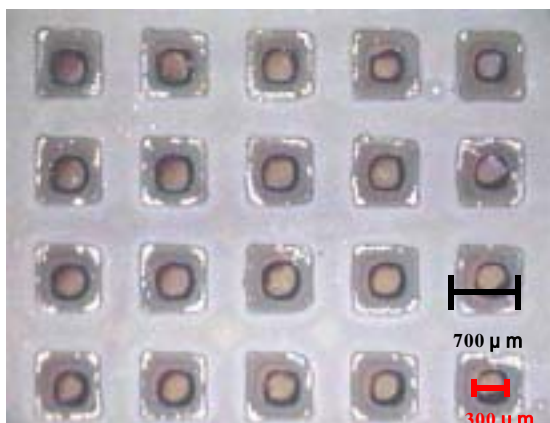


Fig. 9 SEM image for the patterned PZT/LNO thin film capacitor deposited on the Sib wafer.

### 3.5 Characterization of Patterned PZT/LNO Thin Film Capacitor

By using both thiol SAM and OTS SAM, we successfully deposited patterned PZT/LNO thin film capacitor. Then, we measured the electrical properties of the resulting thin film capacitors. Figures 10 and 11 exhibit the dielectric and ferroelectric properties of the resultant PZT/LNO thin film capacitor to compare with those for the non-patterned and patterned PZT thin films..

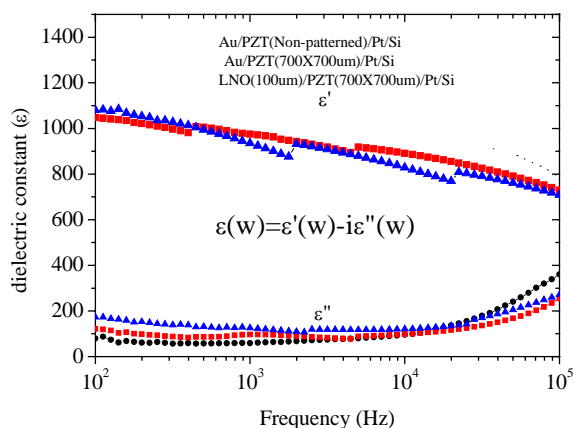


Fig. 10 Dielectric behavior of the patterned PZT/LNO thin film capacitor, together with non-patterned and patterned PZT thin films.

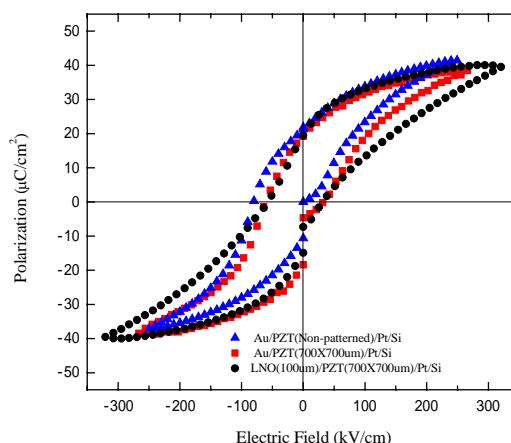
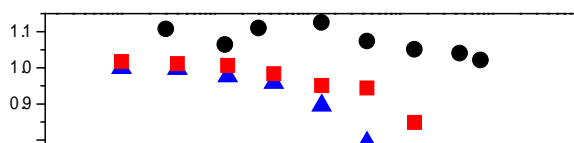


Fig. 11 Ferroelectric properties for the patterned PZT/LNO thin film capacitors compared with that for the non-patterned PZT thin films.

As can be seen in figures, all these properties were almost same for these thin films. This demonstrated that use of SAM as a template was very easy and powerful method for micro-patterning of the CSD-derived thin films.

Figure 12 shows the fatigue behaviors for the patterned PZT/LNO thin film capacitor together with those for the non-patterned and patterned PZT thin films. As it was expected, the normalized remanent



polarization for the non-patterned and patterned PZT films with metal electrode catastrophically degraded at around  $10^6$  switching cycles.

Fig. 12 Change in normalized remanent polarization for the patterned PZT and PZT/LNO thin film capacitors with switching cycles, together with that for the non-patterned PZT thin films.

On the other hand, normalized remanent polarization for the PZT/LNO thin film capacitor did not change over the  $10^8$  switching cycles. From these results, it was concluded that micro-patterning of PZT/LNO oxide electrode thin films were very promising for the nano-devices such as actuated mirror array and the ultra-thin electron emission source for display.

#### 4. Conclusions

By using  $\text{CF}_3(\text{CF}_2)_5\text{C}_{13}\text{H}_{24}\text{O}_2\text{SH}$  as a SAM molecule, patterned PZT film with a MPB composition was successfully deposited in micrometer size easily through all wet processing. The resulting PZT micro-pattern exhibited almost same and excellent dielectric and ferroelectric properties as those for the non-patterned PZT film. Therefore, it is concluded that patterning by using thiol SAM is very promising for a novel processing not only for PZT but also other films with CSD. We also deposited the patterned LNO oxide electrode thin films on the patterned PZT thin films by using OTS SAM. LNO oxide electrode thin film dramatically improved the fatigue property of the patterned PZT thin films.

#### 5. Acknowledgements

This work was supported in part by Grants-in-Aid for Scientific Research (B) (No.16360325) from Japan

Society for the Promotion of Science.

#### 6. References

- [1] B. Jaffe, W. R. Cook, and H. Jaffe, *Piezoelectric Ceramics* (Academic Press, London, 1971).
- [2] D. Damijanovic, *Rep. Prog. Phys.*, **61**, 1267 (1988).
- [3] X. H. Du, J. Zheng, U. Belegundu, and K. Uchino, *Appl. Phys. Lett.*, **72**, 2421 (1988).
- [4] L. Bellaiche and D. Vanderbilt, *Phys. Rev. Lett.*, **83**, 1347 (1999).
- [5] R. Guo, L. E. Cross, S. E. Park, B. Noheda, D. E. Cox, and G. Shirane, *Phys. Rev. Lett.* **84**, 5423 (2000).
- [6] B. Noheda, D. E. Cox, G. Shirane, R. Guo, B. Jones, and L. E. Cross, *Phys. Rev. B* **63**, 14103 (2000).
- [7] H. Kueppers, T. Leuerer, E. Monkwa, *Sensors & Actuators, A* **97-98**, 680 (2002).
- [8] R. Suchanek, R. Tews, G. Gerlach, *Surface & Coatings Technology*, **116-119**, 456 (1999).
- [9] J. Akiwase, *Ouyoubuturi*, **68**, No.1, (1999).
- [10] M. Alexe, C. Haragea, A. Visinoiu, *Scripta Mater.*, **44**, 1175 (2000).
- [11] K. Li, D. W. Zeng, K. C. Yung, *Mater. Chem. Physics*, **75**, 147-150 (2002).
- [12] A. Ulman, *Chem. Rev.*, **96**, 1533 (1996).
- [13] H. Suzuki, M. B. Othoman, K. Murakami, S. Kaneko, T. Hayashi, *Jpn. J. Appl. Phys.*, **35**, [9B] 4896 (1996).
- [14] H. Miyazaki, T. Goto, Y. Miwa, T. Ohno, H. Suzuki, T. Ota, M. Takahashi, *J. Europ. Ceram. Soc.*, **24**, 1005 (2004).
- [15] C. D. Bain, E. B. Troughton, *J. Am. Chem. Soc.*, **111**, 321 (1989).
- [16] G. M. Whitesides, P. E. Labinis, *Langmuir*, **6**, 87 (1990).
- [17] L. H. Dubois, R. G. Nuzzo, *Ann. Rrv. Phys. Chem.*, **43**, 437 (1992).
- [18] H. Sugimura, O. Takai, *Surface Science*, **22**, No.6, 364 (2001).
- [19] H. Suzuki, Y. Kondo, S. Kaneko, T. Tsutsumi, T. Miura and T. Hayashi, *Mat. Res. Soc. Symp. Proc.* **495**, 245 (1998)

